Neurobiology of Disease 184 (2023) 106195

Contents lists available at ScienceDirect

Neurobiology of Disease

journal homepage: www.elsevier.com/locate/ynbdi

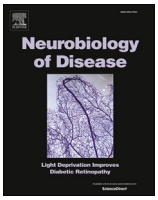

Thyroid hormone transporter Mct8/Oatp1c1 deficiency compromises proper oligodendrocyte maturation in the mouse CNS

Steffen Mayerl *, Heike Heuer

Dept. of Endocrinology, Diabetes & Metabolism, University of Duisburg-Essen, Essen, Germany

ARTICLE INFO

Keywords:
Myelin
Mct8
Oatp1c1
Oligodendroglia
Thyroid hormone
T4
T3
Slc16a2
Slco1c1
CNS

ABSTRACT

Proper CNS myelination depends on the timed availability of thyroid hormone (TH) that induces differentiation of oligodendrocyte precursor cells (OPCs) to mature, myelinating oligodendrocytes. Abnormal myelination is frequently observed in Allan-Herndon-Dudley syndrome caused by inactivating mutations in the TH transporter MCT8. Likewise, persistent hypomyelination is a key CNS feature of the Mct8/Oatp1c1 double knockout (Dko) mouse model, a well-established mouse model for human MCT8 deficiency that exhibits diminished TH transport across brain barriers and thus a TH deficient CNS. Here, we explored whether decreased myelin content is caused by an impairment in oligodendrocyte maturation. To that end, we studied OPC and oligodendrocyte populations in Dko mice versus wild-type and single TH transporter knockout animals at different developmental time points (at postnatal days P12, P30, and P120) using multi-marker immunostaining and confocal microscopy. Only in Dko mice we observed a reduction in cells expressing the oligodendroglia marker Olig2, encompassing all stages between OPCs and mature oligodendrocytes. Moreover, Dko mice exhibited at all analysed time points an increased portion of OPCs and a reduced number of mature oligodendrocytes both in white and grey matter regions indicating a differentiation blockage in the absence of Mct8/Oatp1c1. We also assessed cortical oligodendrocyte structural parameters by visualizing and counting the number of mature myelin sheaths formed per oligodendrocyte. Again, only Dko mice displayed a reduced number of myelin sheaths that in turn exhibited an increase in length indicating a compensatory response to the reduced number of mature oligodendrocytes. Altogether, our studies underscore an oligodendrocyte differentiation impairment and altered oligodendrocyte structural parameters in the global absence of Mct8 and Oatp1c1. Both mechanisms most likely do not only cause the abnormal myelination state but also contribute to compromised neuronal functionality in Mct8/Oatp1c1 deficient animals.

1. Introduction

Myelination is pivotal for proper CNS function as myelin sheaths enable a fast signal propagation along axons, and further provide metabolic support to the insulated axonal compartments. Due to these critical functions, impairments in the development of oligodendrocytes and thus CNS myelination have devastating consequences for neural connectivity, neurological performance and motor coordination (Alizadeh et al., 2015). Thyroid hormone (TH) constitutes a critical external signalling cue that coordinates oligodendrocyte generation from oligodendrocyte progenitor cells (OPCs) and also directly controls myelin formation. Consequently, inadequate levels of TH during development result in delayed myelination, diminished myelin deposition and an overall reduction in the number of myelinated axons (Bernal, 2005).

In order to promote proper myelination inside the CNS, TH has to cross the blood-brain-barrier and enter oligodendrocytes. Thus, intracellular TH action requires the presence of transmembrane transporters of which the highly specific monocarboxylate transporter MCT8 represents the most prominent example. Inactivating mutations in the MCT8 encoding *SLC16A2* gene cause Allan-Herndon-Dudley syndrome (AHDS), a disease that is characterized by severe motor impairments, intellectual deficits and neurological symptoms including an abnormal myelination (Dumitrescu et al., 2004; Friesema et al., 2004; Schwartz et al., 2005; Groeneweg et al., 2017; Van Geest et al., 2021). Of note, different mutations in the *SLC16A2* gene confer various degrees of severity ranging from relatively mild to profound impairments and may thus affect the myelination pattern differently (Remerand et al., 2019). The neurological and motor symptoms of AHDS patients are

* Corresponding author at: University Hospital Essen, Hufelandstraße 55, 45147 Essen, Germany.
E-mail address: steffen.mayerl@uk-essen.de (S. Mayerl).

https://doi.org/10.1016/j.nbd.2023.106195
Received 18 April 2023; Received in revised form 26 May 2023; Accepted 7 June 2023
Available online 10 June 2023

accompanied by abnormal serum TH parameters and thyrotoxic symptoms in peripheral tissues suggesting that MCT8 is critical for the TH transport into the brain and neural target cells. This hypothesis is substantiated by Mct8 knockout mice, which replicate the peripheral phenotype of MCT8 patients and exhibit a diminished transport of the active hormone T3 into the CNS (Dumitrescu et al., 2006; Trajkovic et al., 2007). Yet, due to the presence of the T4-specific organic anion transporting protein Oatp1c1 at the murine blood-brain barrier, T4 can still enter the CNS where it is locally converted to the active hormone T3. Thus, only mice with a combined inactivation of Mct8 and Oatp1c1 (Dko mice) exhibit a severe state of TH deficiency in the CNS and show a persistent hypomyelination probably due to a reduced expression of TH-regulated myelin associated proteins (Mayerl et al., 2014). Moreover, Mct8 and Oatp1c1 transcripts were found in significant amounts in OPCs, but not in mature oligodendrocytes in the mouse brain (Zhang et al., 2014; Bernal et al., 2015). Yet, to which extent Mct8 and/or Oatp1c1 deficiency cell-autonomously or non-cell-autonomously affect OPC generation and maturation has not been addressed.

In mice, OPCs are generated in three sequential waves between embryonic day 12.5 (E12.5) and postnatal day 0 (P0) from different brain areas from which they migrate out to populate the entire brain (Cristobal and Lee, 2022). Though these three populations exhibit specific spatio-temporal trajectories, they all follow the same, tightly regulated differentiation program through the oligodendroglia lineage that can be followed by analysing cell-stage dependent markers. The maturation process comprises the differentiation of Pdgf receptor alpha (Pdgfra; CD140a) immunopositive OPCs to pre-myelinating oligodendrocytes that then form protrusions to contact multiple axons giving these cells a highly branched morphology. The majority of these pre-myelinating oligodendrocytes undergoes apoptosis, while only a minor percentage is able to complete differentiation to mature, CC1 expressing, myelinating oligodendrocytes that form compact myelin (Hughes et al., 2018; Hughes and Stockton, 2021). Of note, only a portion of OPCs differentiate into mature oligodendrocytes while a distinct pool of precursor cells remains present even in the adult brain where they can be activated on demand and are thus critical players underlying brain plasticity and myelin repair (Cristobal and Lee, 2022; Alizadeh et al., 2015).

Here, we addressed to which extent the global absence of the TH transporters Mct8 and/or Oatp1c1 interferes with the proper differentiation of OPCs to mature oligodendrocytes and the formation of myelin. To this end, we performed an analysis of different oligodendroglia lineage populations in these TH transporter knockout mice at different postnatal time points encompassing the period when myelination peaks out (postnatal days P12 and P30) as well as in adulthood (P120). Our findings revealed an increased OPC pool size in Dko mice. Likewise, only in Dko mice we observed a persistently decreased number of mature oligodendrocytes suggesting a differentiation block in the absence of both TH transporters. Finally, we assessed the amount of myelin formed per single mature oligodendrocytes and found altered structural oligodendrocyte parameters only in Dko mice. Altogether, our findings suggest that Mct8/Oatp1c1 deficiency compromises proper myelination in multiple ways.

2. Material and methods

2.1. Animals

All animal studies were executed in accordance with the European Union (EU) directive 2010/63/EU on the protection of animals used for scientific purposes and in compliance with local regulations by the Animal Welfare Committee of the Landesamt für Natur, Umwelt und Verbraucherschutz Nordrhein-Westfalen (LANUV; Recklinghausen, Germany; approval codes AZ81–02.04.2021.A059 and AZ81–02.04.2022.A156).

Wildtype (Wt), Mct8ko (M8ko), Oatp1c1ko (O1ko), and Dko mice on a C57BL/6 background were bred and genotyped as described elsewhere (Trajkovic et al., 2007; Mayerl et al., 2012; Mayerl et al., 2014). Animals were housed under a 12 h light, 12 h dark cycle at constant temperature (22 °C) and were provided with standard laboratory chow and water ad libitum. Mice were subjected to intracardial perfusion-fixation with 4% paraformaldehyde in PBS (4% PFA) under deep ketamine/xylazine-induced anesthesia at postnatal day 12 (P12), at one month (P30) or four months (P120) of age. While for the latter time points only male mice were employed, males and females were used at P12. For EdU labelling studies, mice at P11 and P120 were i.p. injected with EdU (40 μg per g body weight; 10 mg/ml stock; MerckMillipore) and subjected to terminal perfusion as described above. Brains were isolated, post-fixed in 4% PFA for 24 h, cryo-protected with 30% sucrose, snap-frozen in isopentane on dry ice and stored at −80 °C. For quantitative analysis of myelinating oligodendrocytes, one-month-old male mice were deeply anaesthetized by ketamine/xylazine application and intracardially perfused with 4% PFA. Brains were post-fixed and stored at 4 °C in PBS containing 0.4% NaN_3.

2.2. Immunofluorescence studies

Coronal forebrain cryosections (16 μm) collected between Bregma 1.045 and 0.38 were thaw-mounted on superfrost slides, post-fixed with 4% PFA for 10 min and permeabilized with 0.1% Triton X-100/0.1 M glycine. EdU click-it reaction was carried out following the manufacturer's instructions using the Click-iT® EdU Alexa Fluor® 647 Imaging Kit (Thermo Fisher Scientific). Sections were blocked with MOM reagent (1:40; Vector laboratories) in blocking buffer (PBS containing 10% goat or donkey serum and 0.2% Triton X-100) and incubated with the respective primary antibodies in blocking buffer overnight at 4 °C. After washing with PBS, sections were incubated with Alexa Fluor 488, 555, or 647-labelled secondary antibodies raised in goat or donkey (Invitrogen; 1:1000) and with Hoechst33258 (1:10.000, Invitrogen) to label cell nuclei in blocking buffer. After mounting with Fluoromount (Sigma-Aldrich) sections were analysed using a Leica SP8 confocal microscope. For quantification, pictures were taken from the corpus callosum between midline and cingulum bundle as a white matter region and from the adjacent deep cingulate and motor cortex layers as grey matter area.

Quantitative analysis of myelinating oligodendrocytes was carried out according to published protocols (Swire and Ffrench-Constant, 2020; Swire et al., 2019). In brief, 4% PFA-fixed brains were cut into 100 μm thick sections containing the medial prefrontal cortex using a vibratome (Leica). Antigen retrieval was performed at 95 °C for 20 min in 10 mM citrate buffer containing 0.05% Tween20 (pH 6). Sections were washed in PBS, blocked and immunostained as above, transferred onto superfrost slides and mounted using Fluoromount (Sigma-Aldrich). Myelinating oligodendrocytes were imaged in layers II-III of the mouse cortex using a Leica SP8 confocal microscope at 63× magnification and taking z-stacks covering the entire section's thickness. Only those oligodendrocytes whose cell bodies were in the middle third of a section were imaged.

The following primary antibodies were used: mouse anti-APC(CC1) (1:250; Abcam), rabbit anti-Cleaved Caspase-3 (Asp175) (1:250; Cell Signalling Technology), rabbit anti-Caspr (1:250; Abcam), mouse anti-CNP (1:2000; Atlas Antibodies), mouse anti-Gfap (1:500; Sigma), rabbit anti-Iba1 (1:500; Alpha Laboratories), rabbit anti-Ki67 (1:250; Abcam), mouse anti-Olig2 (1:250; Millipore), rabbit anti-Olig2 (1:500; Atlas Antibodies), goat anti-Pdgfr-alpha (1:100; R&D Systems), and goat anti-Sox9 (1:500; R&D Systems).

2.3. Quantifications

All images were processed and analysed using ImageJ software (NIH). Blinding was archived by attributing random numbers to the pictures followed by unblinding after the completion of the respective quantification. Oligodendroglia cell populations were enumerated in

grey and white matter areas and cell numbers were normalized to the measured area. Four mice per genotype and time point were analysed as biological replicates and four pictures per animal were used for quantification. The simple neurite tracer function was utilized to analyse myelinating CNPase immunopositive oligodendrocytes. Originating from the cell body, weakly stained fine processes were traced to much more intensively stained myelin sheaths, whose total length were measured. Caspr staining was used to validate the ends of myelin sheaths (not shown). All fine protrusions were traced allowing for enumeration of the number of myelin sheaths formed per cell. Seven oligodendrocytes were assessed per mouse employing six mice per genotype as biological replicates.

2.4. Statistics

Using Gpower3.1, a priori power calculation was performed based on previous data on Mbp immunofluorescence in Dko mice (Mayerl et al., 2014) indicating that a minimum number of four animals per genotype and time point was required.

All data represent mean ± SD. Statistical significance between Wt, Mct8ko, Oatp1c1ko, and M/Odko mice was determined by two-way ANOVA followed by Tukey post hoc testing. Differences were considered significant when $p < 0.05$ and marked as follows: *, $p < 0.05$; **, $p < 0.01$; ***, $p < 0.001$.

3. Results

3.1. Differentiation impairments in the oligodendroglia lineage in Mct8/Oatp1c1 deficiency

Mct8/Oatp1c1 deficient mice exhibit reduced myelination, which may be caused by a compromised oligodendrocyte development. To test this hypothesis, we determined the overall number of oligodendroglia cells by counting cells immunopositive for the lineage marker Olig2 in Mct8 and/or Oatp1c1 ko animals at different postnatal time points (P12, P30 and P120). We specifically focussed on the corpus callosum as a prominent white matter tract (Fig. 1A,B) and on adjacent cortical areas as grey matter regions (Suppl.Fig. 1). Though Olig2 defines a subset of neural stem cells in the subventricular zone and is further a marker of the pMN motor neuron domain of the spinal cord, it exclusively labels oligodendroglia cells in our regions of interest (Del Aguila et al., 2022; Tan et al., 2014). While at P12 no differences in the oligodendroglia pool

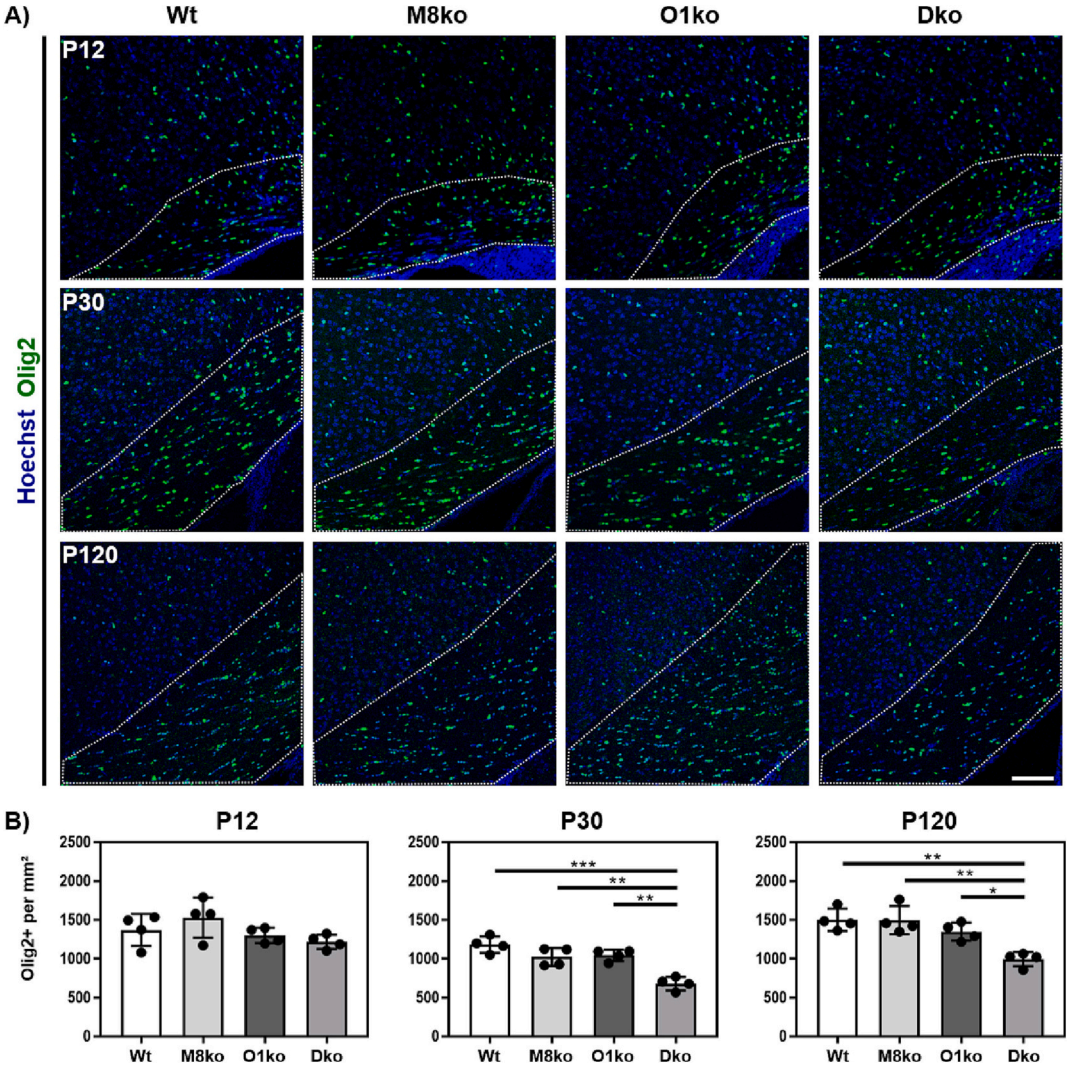

Fig. 1. Oligodendroglia cell pool in Mct8/Oatp1c1 deficiency in mice.
Immuno-histochemical analysis of the lineage marker Olig2. (A) Representative images showing the distribution of Olig2+ cells (in green) in the corpus callosum (enframed area) and adjacent cortical grey matter in Wt, M8ko, O1ko and Dko mice at different developmental time points. Cell nuclei were stained with Hoechst33258 and appear in blue. (B) Enumeration of Olig2+ cell in the white matter area. Absolute numbers were counted and are depicted as density per area. Scale bar: 100 μm. $n = 4$ mice per genotype and time point. *$p < 0.05$, **$p < 0.01$, ***$p < 0.001$.

between the genotypes were visible, a strikingly lower number of Olig2 positive cells was apparent in Dko mice at P30 and P120 both in grey and white matter regions (Fig. 1B and Suppl.Fig. 1). This finding suggests an impairment in the formation and maturation of cells within the oligodendroglia lineage only in Dko animals.

In order to investigate whether these differences are due to an altered proliferative capacity of oligodendroglia cells, we next performed co-staining against Olig2 and the proliferation marker Ki67 (Fig. 2A). Enumerating Olig2/Ki67 double positive cells at P12 revealed similar numbers of proliferating cells in all mouse models both in white and grey matter (Fig. 2B and Suppl.Fig. 2A). Overall proliferation decreased as expected with age, while values remained similar between the different genotypes, both at P30 and P120. We also tested whether augmented apoptosis could explain the drop in total Olig2 numbers specifically in Dko mice. For this purpose, we assessed the apoptotic marker active Caspase 3 (aCasp3) in Olig2 immuno-reactive cells (Fig. 2C). The highest number of aCasp3/Olig2 positive cells were found at P12 whereas at later time points, only very few double positive cells could be detected in the corpus callosum as well as in cortical regions. At all analysed time points, the numbers of apoptotic Olig2 positive cells were not different between all experimental groups. Collectively, these results exclude aCasp3-mediated apoptosis as a potential mechanism for the reduced numbers of Olig2+ cells in Dko mice. We also monitored Iba1 positive microglia cells in P30 old mice and found increased numbers in white matter regions of Dko mice pointing to an ongoing active phagocytic clearance in the corpus callosum (Suppl.Fig. 3A and C). Likewise, we observed elevated astrocyte numbers in Dko mice at P30 in the white matter only (Suppl.Fig. 3B and D) suggesting gliosis in this area. Whether these observations are indicative of an increased non-apoptotic cell death of Olig2+ cells remains to be investigated.

Next, we reverted to the analysis of specific cell types within the oligodendroglia lineage in order to determine at which maturation stage Olig2+ cells are decreased in Dko mice. OPCs were identified using co-immunostaining against Olig2 and the marker Pdgfra (Fig. 3A). By counting Olig2/Pdgfra double positive cells, we detected similar OPC densities in the corpus callosum in all animal groups both at P12 and at P30 (Fig. 3B). At P120, however, OPC numbers were significantly elevated in Dko mice compared to Wt controls. We then calculated the relative contribution of OPCs to the total Olig2+ pool (Fig. 3C) and found strikingly increased values in Dko mice already at P12. With age, the relative contribution of OPCs to all Olig2+ cells decreased as expected though values in Dko mice remained persistently elevated. Similar observations were made in cortical grey matter regions where we unravelled significantly higher absolute OPC densities at P12 and at P120 (Suppl.Fig. 4). Overall, our observations indicate a higher percentage of OPCs in Dko mice at all analysed time points. To further test for potential differences in the cell cycle that may underlie the observed differences, we performed EdU labelling studies (Suppl.Fig. 5). When injected at P11 and analysed 24 h later at P12, a similar number of EdU-labelled OPCs was found in all genotypes in the corpus callosum indicating that the number of cells in S-phase, during which EdU is incorporated, was similar between Dko and control mice (Suppl.Fig. 5A and B). Moreover, the number of apoptotic Olig2/EdU/aCasp3 triple positive cells was not significantly different between all genotypes (Suppl. Fig. 5C). Likewise, at P120, a similar number of EdU-labelled OPCs was detected in all genotypes 24 h after label injection (Suppl.Fig. 5D). Given the increased number of OPCs at that time point, a lower proliferative capacity of OPCs in the Dko brain can be hypothesized.

To next assess mature oligodendrocytes, we employed co-immunostaining against Olig2 and the marker Quaking 7/adenomatous polyposis coli clone (CC1) which is specifically expressed in myelinating oligodendrocytes (Bin et al., 2016). (Fig. 4A). At all time points, we observed similar numbers of Olig2/CC1 immunopositive cells in Wt and single TH transporter knockout groups in corpus callosum areas (Fig. 4B), whereas Dko mice exhibited a 50% reduction in mature oligodendrocytes at P12 and P30 and a 65% reduction at P120 compared to Wt controls. We also calculated the relative contribution of mature oligodendrocytes to the total Olig2+ cell pool (Fig. 4C). As with absolute cell numbers, the relative contribution of Olig2/CC1+ cells was decreased in the corpus callosum of Dko mice reaching only 50% of the Wt level at P12 and being consistently lower at later time points. In grey matter regions, we also observed continuously lower mature oligodendrocyte numbers in cortical areas of Dko mice although the phenotype was less profound as in white matter areas (Suppl.Fig. 6). In sum, persistently elevated OPC numbers and reduced mature oligodendrocyte densities point to lineage progression (i.e. differentiation) impairments in Dko animals throughout postnatal development.

3.2. Grey matter oligodendrocytes of Dko mice exhibit altered myelin sheath formation

Finally, we wondered whether the reduced number of mature oligodendrocytes in Dko mice is partially compensated by an increased myelin formation by the residual oligodendrocytes. To assess this, we employed a recent protocol that enabled us to quantify the number of myelin sheaths formed by individual oligodendrocytes and their respective lengths based on CNPase immunoreactivity without the need for reporter mice (Swire et al., 2019; Swire and Ffrench-Constant, 2020). We conducted our analysis in layers II-III of the medial prefrontal cortex in one-month-old mice as the local sparse myelination facilitates the identification of single oligodendrocytes and the correct assignment of mature myelin sheaths (Fig. 5A). In Wt mice, oligodendrocytes produced a mean number of 45 myelin sheaths per cell (45.09 $\pm$ 2.14 sheaths) with an average length of 46.33 $\pm$ 3.00 µm (Fig. 5B and C, respectively). These values are well within the range of previously reported parameters for Wt mice stressing the robustness of this analysis (Swire et al., 2019). While M8ko and O1ko mice displayed similar values as Wt animals, mean myelin sheath number was reduced to 38.60 $\pm$ 5.33 sheaths in Dko mice (Fig. 5B). In contrast, average sheath length was increased to 55.85 $\pm$ 3.29 µm in Dko mice (Fig. 5C). This general increase is also reflected in the frequency distribution (Fig. 5D) showing a qualitative shift in the distribution curve to longer lengths only in Dko mice though no statistical analysis has been performed. Together, these results demonstrate that quantitative parameters of myelin sheaths are altered in Dko mice, which adds another layer of complexity to their abnormal myelin phenotype with putatively severe consequences for network functionality.

4. Discussion

Inactivating mutations in MCT8 result in AHDS, a severe form of psychomotor disability that is characterized by abnormal serum TH levels and symptoms reminiscent of a central TH deficit (Friesema et al., 2004; Dumitrescu et al., 2004; Schwartz et al., 2005; Groeneweg et al., 2017). Patients exhibit hypomyelination in magnetic resonance imaging (MRI) studies, particularly at a young age (as recently reviewed in (Vancamp et al., 2020, Iwayama et al., 2021)). Such a phenotype is present in 84% of patients $\leq$2 years of age, while only 33% of patients older than 6 years of age still demonstrate an abnormal myelination in MRI tests thus arguing for a generally slow, but increment improvement in the myelin status. This, however, may also depend on the specific mutation in the *SLC16A2* gene and its impact on MCT8 mediated TH transmembrane transport, as the various mutations known result in different degrees of neurological impairments (Remerand et al., 2019). Mild mutations may thus confer a better improvement in the myelin content than mutations resulting in a severe phenotype and that may strongly impair proper myelination. Importantly, there are some patients who never exhibit a normalization in MRI data and hence never acquire normal white matter content even above the age of 10 years (Vancamp et al., 2020). Due to these discrepancies in available MRI data, the debate whether myelination in AHDS is only delayed or permanently compromised is ongoing. However, the difference between

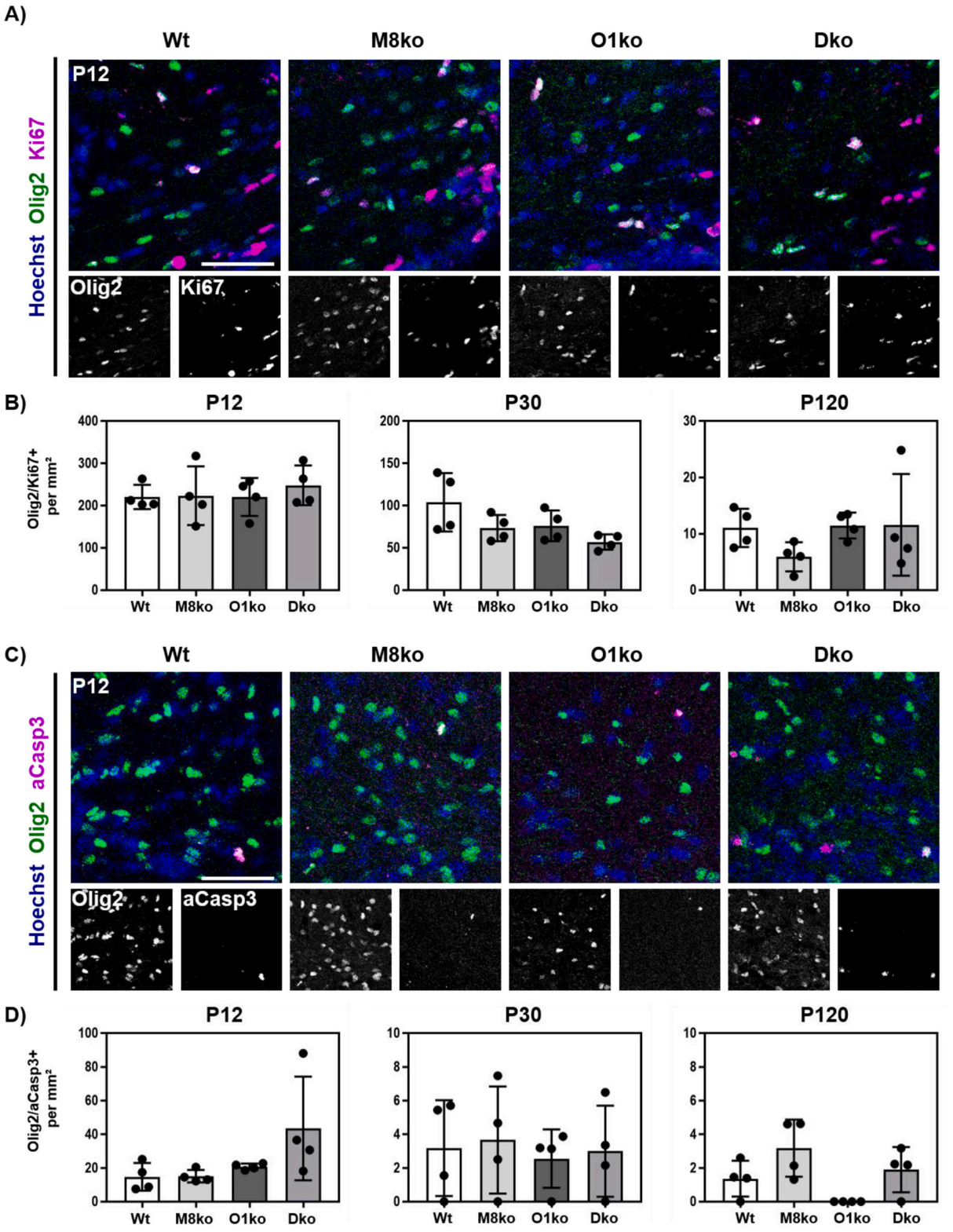

Fig. 2. Oligodendroglia proliferation and apoptosis in TH transporter deficient mice.
Cryosections derived from perfusion-fixed mouse brains were subjected to immunostaining. (A) Proliferative capacity of oligodendroglia cells was determined by Olig2 (in green)/ Ki67 (in magenta) co-staining. Representative pictures in the corpus callosum of P12 mice are shown. Single channel images in grey scale are presented underneath. (B) Olig2/Ki67 double positive cells were counted and their density is presented per time point. (C) Olig2 (in green)/ aCasp3 (in magenta) co-staining to identify Caspase3-dependent apoptosis. Representative pictures from the corpus callosum are shown. Single channel images in grey scale are presented underneath. (D) Calculated densities of Olig2/aCasp3+ cells at the analysed time points. In all immuno-staining, Hoechst33258-labelled cell nuclei are displayed in blue. Scale bars: 50 μm. $n = 4$ mice per genotype and time point.

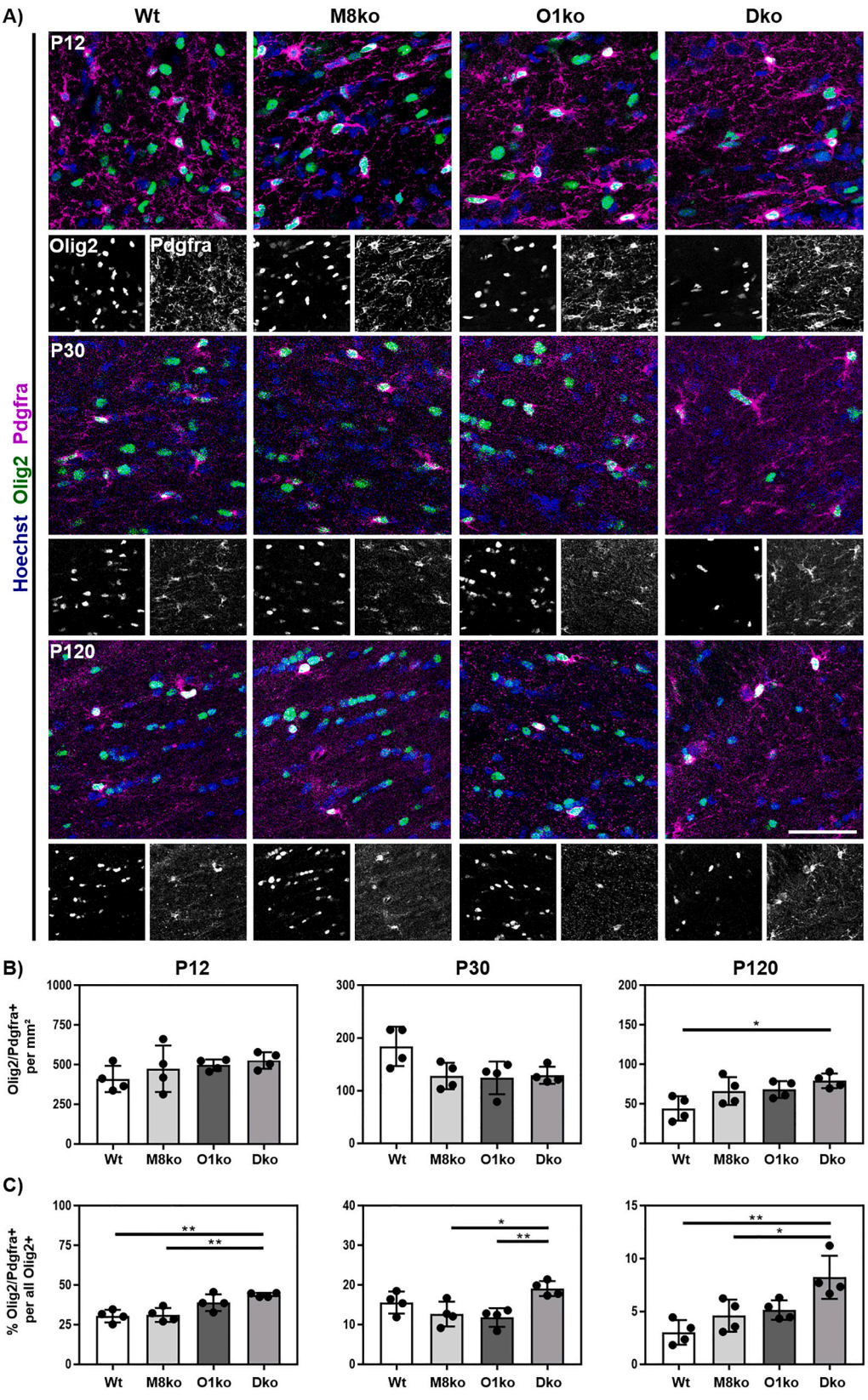

Fig. 3. OPC numbers in TH transporter deficient mice.
(A) Representative images depicting Olig2 (in green)/ Pdgfra (in magenta) double positive OPCs in the corpus callosum of TH transporter deficient mice at different developmental stages. Hoechst33258-labelled cell nuclei are shown in blue. Single channel images for Olig2 and Pdgfra in grey scale are presented underneath. (B) Density of double positive OPCs at different time points is shown based on their absolute cell numbers. (C) Relative contribution of Olig2/Pdgfra positive OPCs to the overall pool of Olig2+ cells per time point. Scale bar: 50 μm. $n = 4$ mice per genotype and time point. $^{*}p < 0.05$, $^{**}p < 0.01$.

the two is very important for AHDS diagnosis and therapy, since delayed myelination might simply be a nonspecific feature of delayed development (Bernal et al., 2015). If constituting a specific feature of AHDS, putative treatment approaches will have to ensure ameliorating effects on the oligodendroglia lineage and myelination as well apart from overcoming TH uptake impairments across the blood-brain barrier (BBB). Post-mortem analysis of an 11-year-old patient revealed reduced MBP immunoreactivity in cerebellar white matter arguing against a nonspecific delay and therefore for a permanent, specific feature of AHDS (Lopez-Espindola et al., 2014). It is thus tempting to speculate

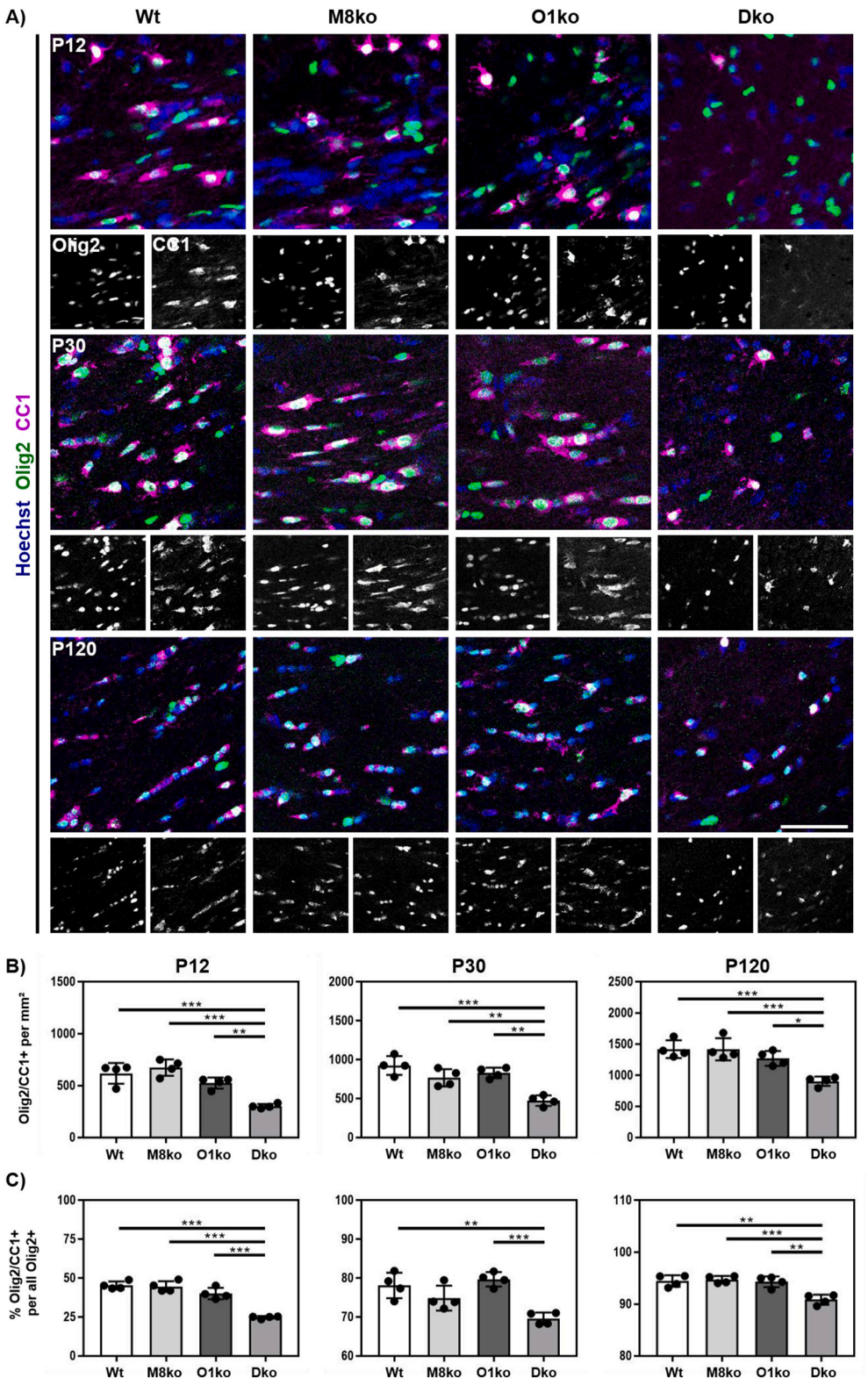

Fig. 4. Mature oligodendrocytes in TH transporter deficient mice.
(A) Representative images assessing Olig2 (in green)/ CC1 (in magenta) double positive mature oligodendrocytes in the corpus callosum in TH transporter deficiency. Cell nuclei were counter-stained with Hoechst33258 and are shown in blue. Single channel images for Olig2 and CC1 in grey scale are depicted underneath. (B) Absolute numbers of Olig2/CC1 double positive cells were counted and are depicted as densities per mm^2 at different time points during postnatal development. (C) Fraction of mature oligodendroglia cells within the total Olig2+ cell pool was calculated for each genotype and time point. Scale bar: 50 μm. $n = 4$ mice per genotype and time point. $^*p < 0.05$, $^{**}p < 0.01$, $^{***}p < 0.001$.

that MRI studies might not always be sensitive enough to detect milder structural alterations in myelin.

Immuno-histochemical and MRI data align in the established AHDS mouse model of Mct8/Oatp1c1 deficiency demonstrating a permanently reduced CNS myelination status as well as reductions in the brain white and grey matter volumes (Mayerl et al., 2014; Reinwald et al., 2022). Moreover, previous electron microscopic (EM) analysis in the corpus callosum highlighted a normal ultrastructure of those myelin sheaths that are generated in Dko mice although the density of myelinated axons was reduced, a fact that further stresses the permanent myelination deficits in this mouse model. The question as to the underlying mechanisms, however, remains elusive. As one possible scenario, the reduced number of myelinated axons could be explained by a lower axon diameter as a certain threshold is required for myelination.

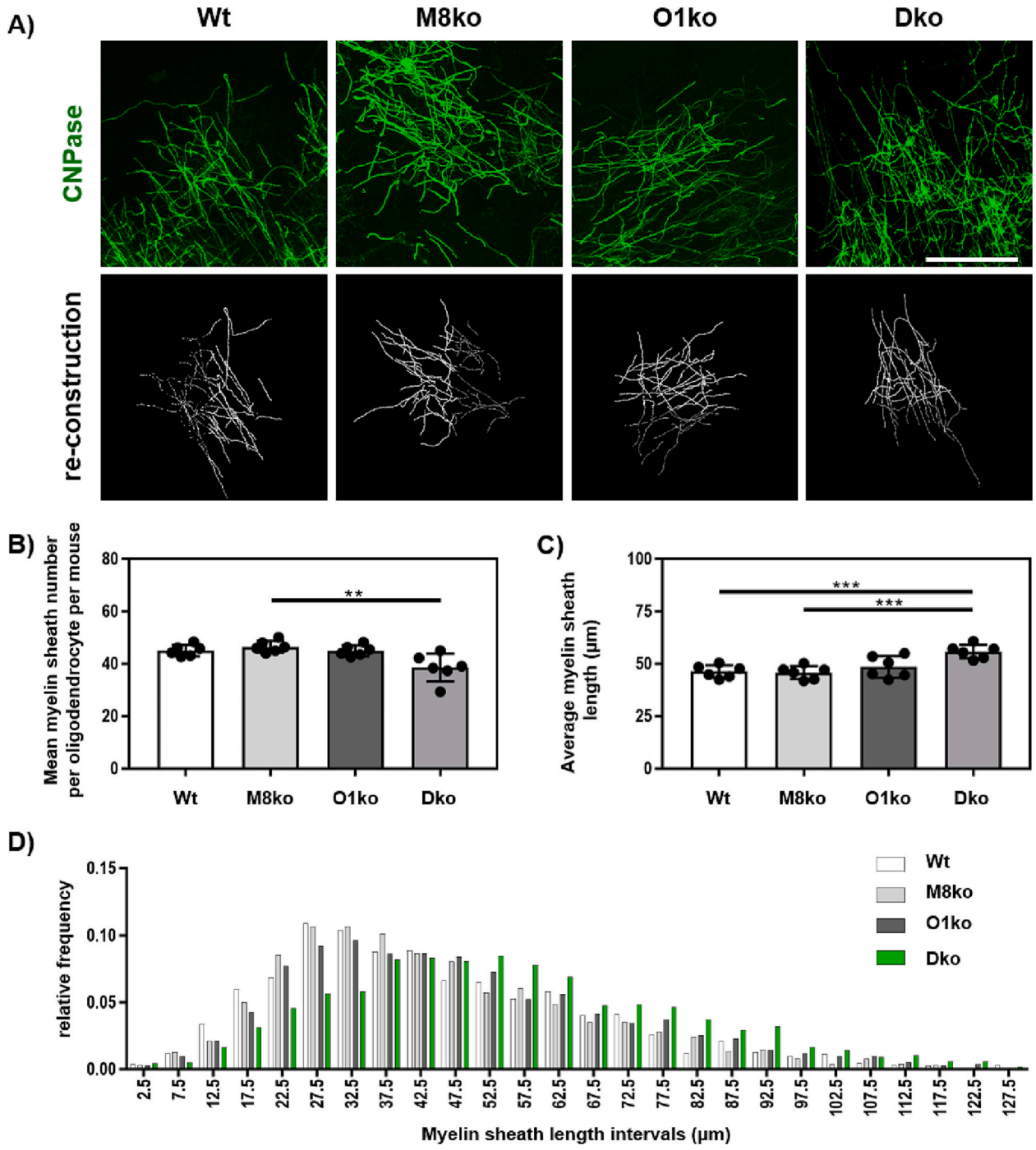

Fig. 5. Mct8/Oatp1c1 Dko alters myelin sheath number and length.
CNPase immuno-staining was conducted to visualize myelinating oligodendrocytes. (A) Representative pictures of CNPase (in green) stained cells in the medial prefrontal cortex of 1-month-old-mice. Pictures are presented as 2D projections of larger z-stacks. All myelin sheaths produced by a single exemplary oligodendrocyte per genotype are depicted in the 2D reconstruction (in grey scale). (B) Number of myelin sheaths produced by individual mature oligodendrocytes was counted. The graph shows the mean number of sheaths per oligodendrocyte per animal. (C) Length of individual myelin sheaths was measured. The graph presents the average length of myelin sheaths over all analysed oligodendrocytes per animal. (D) Myelin sheaths over all oligodendrocytes and animals from the same genotype were sorted according to their length and the frequency distribution of the sorted intervals over all sheaths is shown. Scale bar: 100 µm. $n = 6$ mice per genotype (7 individual oligodendrocytes were assessed per mouse). $^{**}p < 0.01$, $^{***}p < 0.001$.

Alternatively, we put forward the hypothesis that impairments in developmental oligodendroglia maturation leads to insufficient numbers of myelinating oligodendrocytes and are thus a key mechanism causing hypomyelination.

To test our hypothesis, we performed in-depth immuno-histochemical profiling in order to quantify the total number of oligodendroglia cells expressing the transcription factor Olig2 and the respective portion of immature oligodendrocytes precursor cells versus mature myelinating oligodendrocytes in Dko and control mice. We also included Mct8ko and Oatp1c1ko mice in our study as both TH transporter single mutant mice exhibit a distinct phenotype of disturbed TH transport and homeostasis in the CNS (Mayerl et al., 2014). However,

both Mct8ko and Oatp1c1ko mice exhibited a similar composition of OPCs and mature oligodendrocytes as control animals at all analysed time points, which fits very well with a normal myelination pattern as seen in our previous immunohistochemistry studies. In contrast, mice lacking both transporters simultaneously showed significantly reduced numbers of myelinating oligodendrocytes at every analysed time point (Fig. 6). Furthermore, at P30 and thus after the postnatal peak period of myelination is finished, we observed that myelinating oligodendrocytes produced in average fewer but longer myelin sheaths, which matches well our previous EM observation of a reduced number of myelinated axons in Dko mice (Fig. 6). Hence, we demonstrate that the reduced myelination seen in Dko mice is not only the consequence of a decreased production of TH-regulated myelin proteins but also reflects a disturbed oligodendroglia differentiation.

Despite the reduced numbers of mature oligodendrocytes, OPC numbers are unaltered in Dko mice in comparison to controls at P12 and P30 or even elevated at P120. These alterations account for the calculated higher proportion of OPCs that emphasizes the presence of a differentiation blockage in at least a subgroup of these precursor cells (Fig. 6). In this regard, we hypothesize that more OPCs enter the quiescent G0 phase of the cell cycle in Dko mice in response to an impaired differentiation. Such a scenario would explain the similar number of proliferating Olig2+/Ki67+ cells and a similar number of EdU-labelled OPCs in all genotypes despite elevated OPC numbers and a generally lower decline in absolute OPC numbers in Mct8/Oatp1c1 deficient mice with age. Of note, putative alterations in the proportion of pre-myelinating oligodendrocytes remain elusive and should further be assessed using antibodies against stage-specific marker proteins such as Bcas1 (breast carcinoma amplified sequence 1) (Fard et al., 2017).

The central myelination state was recently investigated in Mct8/Dio2 Dko mice, an alternative mouse model for human MCT8 deficiency (Valcarcel-Hernandez et al., 2022; Barez-Lopez et al., 2019). In agreement with our previous findings (Mayerl et al., 2014), Mct8/Dio2 Dko mice show an impaired myelination and a reduced number of myelinated axons in electron microscopic images without alterations in the g-ratio (Valcarcel-Hernandez et al., 2022). In contrast to our results, Mct8/Dio2 Dko mice present with progressive improvements in the white matter content. These differences may be explained by the presence of T4 in the Mct8/Dio2 Dko brain in contrast to Mct8/Oatp1c1 Dko mice and thus a possible direct action of T4 on nuclear TH receptors or by non-genomic effects of T4 binding to the αvβ3 receptor that is present in oligodendroglia cells (Milner and Ffrench-Constant, 1994). In addition, recent single cell RNA sequencing studies highlighted oligodendrocyte maturation impairments upon defective TRα1 signalling pointing to a critical role of TRα1 on oligodendroglia lineage progression (Sreenivasan et al., 2023).

When exactly the differentiation blockage in Mct8/Oatp1c1 deficiency occurs and whether already the cell-fate decision of neural precursor cells is affected needs to be determined further e.g. by conducting lineage tracing studies that allow a close monitoring of distinct oligodendroglia cell populations born at different time points. In the adult mouse subventricular zone, Remaud et al. recently showed that the activation of neural stem cells, their fate decision towards the oligodendroglia lineage and the maturation of newly generated OPCs to myelinating oligodendrocytes requires a fine-tuned intracellular TH signalling. A transient, T3-free window thereby favours the generation of OPCs over neuroblasts from adult stem cells while TH is critical to stimulate differentiation to oligodendrocytes and myelin formation (Remaud et al., 2017). It is therefore conceivable that the absence of Mct8 and Oatp1c1 at prenatal stages already affects embryonic neural stem cells and/or their niche thus altering the balance of neurogenic and glial commitment.

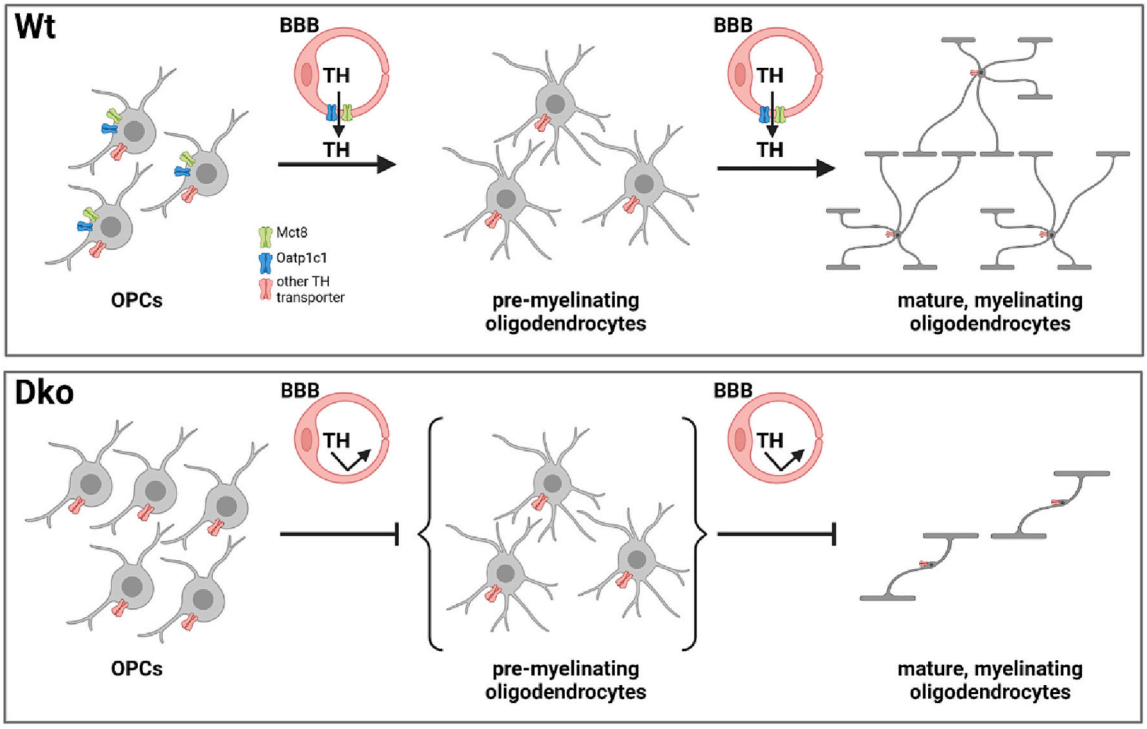

Fig. 6. Model of TH-transporter dependent oligodendroglia lineage progression.
In Wt mice, TH transporters Mct8 and Oatp1c1 mediate TH uptake across BBB endothelial cells into the brain parenchyma. According to RNA sequencing data (Zhang et al., 2014; Bernal et al., 2015), Mct8 and Oatp1c1 are further present in at least subsets of OPC suggesting a role in cellular TH uptake. In the oligodendroglia lineage, TH causes exit from the cell cycle and induces differentiation of OPCs to pre-myelinating and myelinating, mature oligodendrocytes. In Dko mice, absence of Mct8 and Oatp1c1 strongly impairs TH uptake across brain barriers, blocks proper differentiation and results in increased OPC numbers as well as reduced mature oligodendrocyte numbers. Brackets around pre-myelinating oligodendrocytes in Dko mice indicate that putative alterations are still elusive. Individual mature oligodendrocytes generate fewer, but longer myelin sheaths in Dko mice. Graphic was created with Biorender.

How can the decrease in Olig2+ cells in Dko mice after weaning be explained if not by altered proliferation or apoptosis? As one possibility, cell death may occur independently of Caspase 3 activation that was used as a read-out in this study. A recent report emphasized the importance of the Bak/Bax apoptosis checkpoint in the survival of pre-myelinating oligodendrocytes (Hughes and Stockton, 2021). Upon stimulation, Bak/Bax translocate to the mitochondrial membrane, where they provoke depolarization, increase membrane permeability and the release of cleaved AIF (apoptosis inducing factor) that interacts with endonuclease G to cause DNA fragmentation and cell death (Tait and Green, 2013; Bhadra, 2022). Likewise, recent studies have emphasized the susceptibility of oligodendroglia cells to ferroptosis that is driving oligodendrocyte loss and demyelination of EAE- and cuprizone-induced myelin insults (Jhelum et al., 2020; Li et al., 2022). In the future, it will be important to address these alternative cell death mechanisms in more detail. Alternatively, the observed gliosis in the Dko corpus callosum may alter critical extracellular matrix components and thus hamper oligodendroglia maturation. Astrocytes for instance secrete hyaluronan, which inhibits OPC differentiation and promotes astrocytic differentiation and whose elevated levels play a major role in certain leukodystrophies such as vanishing white matter disease (Bugiani et al., 2013; Nutma et al., 2020).

As another important question, it remains to be addressed whether the oligodendrocyte maturation defect in Dko mice can be solely attributed to the general TH deficiency in the CNS of these animals or whether both TH transporters additionally exhibit cell-autonomous functions within the oligodendroglia lineage. RNA sequencing of FACS isolated CNS populations derived from the P17 mouse brain revealed the presence of Mct8 and Oatp1c1 in OPCs thus emphasizing a direct role of both TH transporters within the lineage (Bernal et al., 2015; Zhang et al., 2014). It remains to be seen if absence of Mct8/Oatp1c1 from the oligodendroglia lineage interferes with proper differentiation and maturation programs or structural parameters of mature oligodendrocytes. Of note, the regulation of myelin sheath length is an intrinsic feature of oligodendrocytes, but also affected by neuronal activity and synaptic vesicle release (Bechler et al., 2015; Mensch et al., 2015; Hines et al., 2015). The mechanisms by which the average myelin sheath number per oligodendrocyte is reduced in Dko mice is similarly elusive. Recently, the endothelin signalling pathways was highlighted as a potent regulator of myelin sheath number (Swire et al., 2019). How impairments in neuronal development and connectivity or alterations in brain endothelial cells contribute to the observed structural abnormalities of mature oligodendrocytes in global Mct8/Oatp1c1 deficiency requires a more detailed analysis using conditional knockout approaches for both TH transporters in neuronal, endothelial, and oligodendroglia cells.

The aspect of cell-autonomous functions of Mct8 and Oatp1c1 is also of translational relevance as novel therapeutic strategies for AHDS patients aim to restore TH transporter function specifically at brain barriers (Sundaram et al., 2022; Liao et al., 2022). By exploiting a gene therapy approach, Sundaram et al. recently achieved Mct8 re-expression in blood-brain barrier (BBB) endothelial cells of Dko mice after neonatal injection of an AAV-BR1-Mct8 construct and reported increased brain T3 content and improvement of several neuronal differentiation markers (Sundaram et al., 2022). Yet, numbers of mature, CC1 positive oligodendrocytes remained low suggesting that apart from their critical role at the BBB the TH transporters Mct8/Oatp1c1 additionally exert cell-intrinsic functions within the oligodendroglia lineage. Future studies of mice lacking both TH transporters solely in oligodendroglia cells will certainly clarify this aspect.

Does a compromised oligodendroglia differentiation also occur in human MCT8 deficiency? Post-mortem analysis of brain tissue from a MCT8 patient revealed a persistently abnormal myelination in comparison to an age-matched control as based on reduced MBP staining and Luxol Fast Blue staining intensities, a classical myelin staining method, in cerebral and cerebellar sections (Lopez-Espindola et al., 2014; Valcarcel-Hernandez et al., 2022). Whether this is indeed linked to impaired oligodendroglia differentiation remains to be seen as so far, no quantitative analysis has been performed. Recent studies underscored the potential of MCT8 in regulating human oligodendroglia differentiation. In vitro studies that differentiated human embryonic stem cells into oligodendrocytes demonstrated MCT8 immunoreactivity at all stages of lineage development starting with OPCs, while lentivirus-mediated knock-down of MCT8 interfered with proper lineage progression (Lee et al., 2017). Transplantation experiments that assessed the maturation of human iPSC-derived MCT8-deficient and control OPCs in shiverer mouse brains further found a reduced myelination efficiency of MCT8-deficient cells (Vatine et al., 2021). Together, these reports indicate a cell-specific impact of MCT8 for human oligodendrocyte maturation. Thus, impaired oligodendroglia differentiation may indeed constitute a major pathogenic mechanism in AHDS.

5. Conclusions

In this study, we have explored impairments in oligodendroglia lineage differentiation as a putative mechanism for the persistent hypomyelination seen in Mct8/Oatp1c1 Dko mice, a well-established murine model for MCT8 deficiency. We highlight that this hypomyelination is accompanied by a persistent decrease in mature oligodendrocytes both in white and grey matter areas. The concomitant increase in OPCs indicates general differentiation impairments in Dko mice. We further unravelled that myelinating oligodendrocytes generate fewer, but longer myelin sheaths. These structural alterations represent a new and potentially detrimental pathogenic mechanism that may disrupt network synchronisation and thus neuronal circuit functioning. Moreover, our finding advise caution regarding the evaluation of MRI tests in MCT8 deficiency as such structural alterations may be interpreted as "normal" myelin content though on the cellular level myelination is still compromised.

Author contribution

SM and HH devised the experiments and wrote the manuscript. SM performed experiments and conducted the analysis.

Funding

This work was supported by grants of the DFG to SM (CRC/TR296-P19) and HH (CRC/TR296- P09). Funding was further provided by the Sherman Family to HH.

Declaration of Competing Interest

The authors have declared that no conflict of interest exists.

Data availability

Data is available from the corresponding author upon reasonable request.

Acknowledgements

We thank the University Hospital Essen imaging facility (IMCES; Alexandra Brenzel and Anthony Squire) for their support. We further thank Markus Korkowski and Natalie Sadowski for their excellent work.

Appendix A. Supplementary data

Supplementary data to this article can be found online at https://doi.org/10.1016/j.nbd.2023.106195.

References

Alizadeh, A., Dyck, S.M., Karimi-Abdolrezaee, S., 2015. Myelin damage and repair in pathologic CNS: challenges and prospects. Front. Mol. Neurosci. 8, 35.

Barez-Lopez, S., Grijota-Martinez, C., Auso, E., Fernandez-De Frutos, M., Montero-Pedrazuela, A., Guadano-Ferraz, A., 2019. Adult mice lacking Mct8 and Dio2 proteins present alterations in peripheral thyroid hormone levels and severe brain and motor skill impairments. Thyroid 29, 1669–1682.

Bechler, M.E., Byrne, L., Ffrench-Constant, C., 2015. CNS myelin sheath lengths are an intrinsic property of oligodendrocytes. Curr. Biol. 25, 2411–2416.

Bernal, J., 2005. Thyroid hormones and brain development. Vitam. Horm. 71, 95–122.

Bernal, J., Guadano-Ferraz, A., Morte, B., 2015. Thyroid hormone transporters–functions and clinical implications. Nat. Rev. Endocrinol. 11, 406–417.

Bhadra, K., 2022. A mini review on molecules inducing caspase-independent cell death: A new route to Cancer therapy. Molecules 27.

Bin, J.M., Harris, S.N., Kennedy, T.E., 2016. The oligodendrocyte-specific antibody 'CC1' binds quaking 7. J. Neurochem. 139, 181–186.

Bugiani, M., Postma, N., Polder, E., Dieleman, N., Scheffer, P.G., Sim, F.J., Van Der Knaap, M.S., Boor, I., 2013. Hyaluronan accumulation and arrested oligodendrocyte progenitor maturation in vanishing white matter disease. Brain 136, 209–222.

Cristobal, C.D., Lee, H.K., 2022. Development of myelinating glia: an overview. Glia 70, 2237–2259.

Del Aguila, A., Adam, M., Ullom, K., Shaw, N., Qin, S., Ehrman, J., Nardini, D., Salomone, J., Gebelein, B., Lu, Q.R., Potter, S.S., Waclaw, R., Campbell, K., Nakafuku, M., 2022. Olig2 defines a subset of neural stem cells that produce specific olfactory bulb interneuron subtypes in the subventricular zone of adult mice. Development 149.

Dumitrescu, A.M., Liao, X.H., Best, T.B., Brockmann, K., Refetoff, S., 2004. A novel syndrome combining thyroid and neurological abnormalities is associated with mutations in a monocarboxylate transporter gene. Am. J. Hum. Genet. 74, 168–175.

Dumitrescu, A.M., Liao, X.H., Weiss, R.E., Millen, K., Refetoff, S., 2006. Tissue-specific thyroid hormone deprivation and excess in monocarboxylate transporter (mct) 8-deficient mice. Endocrinology 147, 4036–4043.

Fard, M.K., Van Der Meer, F., Sanchez, P., Cantuti-Castelvetri, L., Mandad, S., Jakel, S., Fornasiero, E.F., Schmitt, S., Ehrlich, M., Starost, L., Kuhlmann, T., Sergiou, C., Schultz, V., Wrzos, C., Bruck, W., Urlaub, H., Dimou, L., Stadelmann, C., Simons, M., 2017. BCAS1 expression defines a population of early myelinating oligodendrocytes in multiple sclerosis lesions. Sci. Transl. Med. 9.

Friesema, E.C., Grueters, A., Biebermann, H., Krude, H., Von Moers, A., Reeser, M., Barrett, T.G., Mancilla, E.E., Svensson, J., Kester, M.H., Kuiper, G.G., Balkassmi, S., Uitterlinden, A.G., Koehrle, J., Rodien, P., Halestrap, A.P., Visser, T.J., 2004. Association between mutations in a thyroid hormone transporter and severe X-linked psychomotor retardation. Lancet 364, 1435–1437.

Groeneweg, S., Visser, W.E., Visser, T.J., 2017. Disorder of thyroid hormone transport into the tissues. Best Pract. Res. Clin. Endocrinol. Metab. 31, 241–253.

Hines, J.H., Ravanelli, A.M., Schwindt, R., Scott, E.K., Appel, B., 2015. Neuronal activity biases axon selection for myelination in vivo. Nat. Neurosci. 18, 683–689.

Hughes, E.G., Stockton, M.E., 2021. Premyelinating oligodendrocytes: mechanisms underlying cell survival and integration. Front. Cell Dev. Biol. 9, 714169.

Hughes, E.G., Orthmann-Murphy, J.L., Langseth, A.J., Bergles, D.E., 2018. Myelin remodeling through experience-dependent oligodendrogenesis in the adult somatosensory cortex. Nat. Neurosci. 21, 696–706.

Iwayama, H., Tanaka, T., Aoyama, K., Moroto, M., Adachi, S., Fujisawa, Y., Matsuura, H., Takano, K., Mizuno, H., Okumura, A., 2021. Regional difference in myelination in Monocarboxylate transporter 8 deficiency: case reports and literature review of cases in Japan. Front. Neurol. 12, 657820.

Jhelum, P., Santos-Nogueira, E., Teo, W., Haumont, A., Lenoel, I., Stys, P.K., David, S., 2020. Ferroptosis mediates Cuprizone-induced loss of oligodendrocytes and demyelination. J. Neurosci. 40, 9327–9341.

Lee, J.Y., Kim, M.J., Deliyanti, D., Azari, M.F., Rossello, F., Costin, A., Ramm, G., Stanley, E.G., Elefanty, A.G., Wilkinson-Berka, J.L., Petratos, S., 2017. Overcoming Monocarboxylate transporter 8 (MCT8)-deficiency to promote human oligodendrocyte differentiation and myelination. EBioMedicine 25, 122–135.

Li, X.Y., Chu, Y.J., Ma, R., Dou, M.M., Li, S.L., Song, Y.F., Lv, Y., Zhu, L., 2022. Ferroptosis as a mechanism of oligodendrocyte loss and demyelination in experimental autoimmune encephalomyelitis. J. Neuroimmunol. 373.

Liao, X.H., Avalos, P., Shelest, O., Ofan, R., Shilo, M., Bresee, C., Likhite, S., Vit, J.P., Heuer, H., Kaspar, B., Meyer, K., Dumitrescu, A.M., Refetoff, S., Svendsen, C.N., Vatine, G.D., 2022. AAV9-MCT8 delivery at juvenile stage ameliorates neurological and behavioral deficits in a mouse model of MCT8-deficiency. Thyroid 32, 849–859.

Lopez-Espindola, D., Morales-Bastos, C., Grijota-Martinez, C., Liao, X.H., Lev, D., Sugo, E., Verge, C.F., Refetoff, S., Bernal, J., Guadano-Ferraz, A., 2014. Mutations of the thyroid hormone transporter MCT8 cause prenatal brain damage and persistent hypomyelination. J. Clin. Endocrinol. Metab. 99, E2799–E2804.

Mayerl, S., Visser, T.J., Darras, V.M., Horn, S., Heuer, H., 2012. Impact of Oatp1c1 deficiency on thyroid hormone metabolism and action in the mouse brain. Endocrinology 153, 1528–1537.

Mayerl, S., Muller, J., Bauer, R., Richert, S., Kassmann, C.M., Darras, V.M., Buder, K., Boelen, A., Visser, T.J., Heuer, H., 2014. Transporters MCT8 and OATP1C1 maintain murine brain thyroid hormone homeostasis. J. Clin. Invest. 124, 1987–1999.

Mensch, S., Baraban, M., Almeida, R., Czopka, T., Ausborn, J., El Manira, A., Lyons, D.A., 2015. Synaptic vesicle release regulates myelin sheath number of individual oligodendrocytes in vivo. Nat. Neurosci. 18, 628–630.

Milner, R., Ffrench-Constant, C., 1994. A developmental analysis of oligodendroglial integrins in primary cells: changes in alpha v-associated beta subunits during differentiation. Development 120, 3497–3506.

Nutma, E., Van Gent, D., Amor, S., Peferoen, L.A.N., 2020. Astrocyte and oligodendrocyte cross-talk in the central nervous system. Cells 9.

Reinwald, J.R., Weber-Fahr, W., Cosa-Linan, A., Becker, R., Sack, M., Falfan-Melgoza, C., Gass, N., Braun, U., Clemm Von Hohenberg, C., Chen, J., Mayerl, S., Muente, T.F., Heuer, H., Sartorius, A., 2022. TRIAC treatment improves impaired brain network function and white matter loss in thyroid hormone transporter Mct8/Oatp1c1 deficient mice. Int. J. Mol. Sci. 23.

Remaud, S., Ortiz, F.C., Perret-Jeanneret, M., Aigrot, M.S., Gothie, J.D., Fekete, C., Kvarta-Papp, Z., Gereben, B., Langui, D., Lubetzki, C., Angulo, M.C., Zalc, B., Demeneix, B., 2017. Transient hypothyroidism favors oligodendrocyte generation providing functional remyelination in the adult mouse brain. Elife 6.

Remerand, G., Boespflug-Tanguy, O., Tonduti, D., Touraine, R., Rodriguez, D., Curie, A., Perreton, N., Des Portes, V., Sarret, C., Group, R.A.S., 2019. Expanding the phenotypic spectrum of Allan-Herndon-Dudley syndrome in patients with SLC16A2 mutations. Dev. Med. Child Neurol. 61, 1439–1447.

Schwartz, C.E., May, M.M., Carpenter, N.J., Rogers, R.C., Martin, J., Bialer, M.G., Ward, J., Sanabria, J., Marsa, S., Lewis, J.A., Echeverri, R., Lubs, H.A., Voeller, K., Simensen, R.J., Stevenson, R.E., 2005. Allan-Herndon-Dudley syndrome and the monocarboxylate transporter 8 (MCT8) gene. Am. J. Hum. Genet. 77, 41–53.

Sreenivasan, V.K.A., Dore, R., Resch, J., Maier, J., Dietrich, C., Henck, J., Balachandran, S., Mittag, J., Spielmann, M., 2023. Single-cell RNA-based phenotyping reveals a pivotal role of thyroid hormone receptor alpha for hypothalamic development. Development 150.

Sundaram, S.M., Arrulo Pereira, A., Muller-Fielitz, H., Kopke, H., De Angelis, M., Muller, T.D., Heuer, H., Korbelin, J., Krohn, M., Mittag, J., Nogueiras, R., Prevot, V., Schwaninger, M., 2022. Gene Therapy Targeting the Blood-Brain Barrier Improves Neurological Symptoms in a Model of Genetic MCT8 Deficiency. Brain.

Swire, M., Ffrench-Constant, C., 2020. Staining and quantitative analysis of myelinating oligodendrocytes in the mouse Grey matter. Bio Protoc. 10, e3792.

Swire, M., Kotelevtsev, Y., Webb, D.J., Lyons, D.A., Ffrench-Constant, C., 2019. Endothelin signalling mediates experience-dependent myelination in the CNS. Elife 8.

Tait, S.W., Green, D.R., 2013. Mitochondrial Regulation of Cell Death. Cold Spring Harb Perspect Biol, p. 5.

Tan, B., Yu, J., Yin, Y., Jia, G., Jiang, W., Yu, L., 2014. The Olig family affects central nervous system development and disease. Neural Regen. Res. 9, 329–336.

Trajkovic, M., Visser, T.J., Mittag, J., Horn, S., Lukas, J., Darras, V.M., Raivich, G., Bauer, K., Heuer, H., 2007. Abnormal thyroid hormone metabolism in mice lacking the monocarboxylate transporter 8. J. Clin. Invest. 117, 627–635.

Valcarcel-Hernandez, V., Lopez-Espindola, D., Guillen-Yunta, M., Garcia-Aldea, A., Lopez De Toledo Soler, I., Barez-Lopez, S., Guadano-Ferraz, A., 2022. Deficient thyroid hormone transport to the brain leads to impairments in axonal caliber and oligodendroglial development. Neurobiol. Dis. 162, 105567.

Van Geest, F.S., Groeneweg, S., Visser, W.E., 2021. Monocarboxylate transporter 8 deficiency: update on clinical characteristics and treatment. Endocrine 71, 689–695.

Vancamp, P., Demeneix, B.A., Remaud, S., 2020. Monocarboxylate transporter 8 deficiency: delayed or permanent Hypomyelination? Front. Endocrinol. (Lausanne) 11, 283.

Vatine, G.D., Shelest, O., Barriga, B.K., Ofan, R., Rabinski, T., Mattis, V.B., Heuer, H., Svendsen, C.N., 2021. Oligodendrocyte progenitor cell maturation is dependent on dual function of MCT8 in the transport of thyroid hormone across brain barriers and the plasma membrane. Glia 69, 2146–2159.

Zhang, Y., Chen, K., Sloan, S.A., Bennett, M.L., Scholze, A.R., O'keeffe, S., Phatnani, H.P., Guarnieri, P., Caneda, C., Ruderisch, N., Deng, S., Liddelow, S.A., Zhang, C., Daneman, R., Maniatis, T., Barres, B.A., Wu, J.Q., 2014. An RNA-sequencing transcriptome and splicing database of glia, neurons, and vascular cells of the cerebral cortex. J. Neurosci. 34, 11929–11947.

DOI: 10.1016/j.nbd.2023.106195
URN: urn:nbn:de:hbz:465-20230912-134234-4